Light-Induced Effects on the a-Si H/c-Si Heterointerface

Vasudevan, Ravi; Poli, Isabella; Deligiannis, Dimitris; Zeman, Miro; Smets, Arno

DOI
10.1109/JPHOTOV.2016.2633800

Publication date
2016

Document Version
Accepted author manuscript

Published in
IEEE Journal of Photovoltaics

Light-Induced Effects on the a-Si:H/c-Si Heterointerface

Ravi Vasudevan, Isabella Poli, Dimitrios Deligiannis, Miro Zeman, Arno HM Smets

***Abstract*—Light-induced effects on the minority carrier lifetime of silicon heterojunction structures are studied through multiple exposure photoconductance decay (MEPCD). MEPCD monitors the effect of the measurement flash from a PCD setup on a sample over thousands of measurements. Varying the microstructure of the intrinsic hydrogenated amorphous silicon (a-Si:H) used for passivation of n-type crystalline silicon (c-Si) showed that passivating films rich in voids produce light induced improvement, while denser films result in samples that are susceptible to light induced degradation. Light-induced degradation linked to an increase in dangling bond density at the a-Si:H/c-Si interface while light-induced improvements are linked to charging at the a-Si:H/c-Si interface. Furthermore doped a-Si:H is added to make samples with an emitter and back surface field (BSF). These doped layers have a significant effect on the light-induced kinetics on minority carrier lifetime. Emitter samples exhibit consistent light-induced improvement while BSF samples exhibit light-induced degradation. This is explained through negative charging at the BSF and positive charging at the emitter. Full precursors with a BSF and emitter exhibit different kinetics based on which side is being illuminated. This suggests that the light-induced charging at the a-Si:H/c-Si interface can only occur when a-Si:H has sufficient generation.**

***Index Terms*—Silicon Heteorjunction, a-Si:H, Light-Induced Degradation.**

I. Introduction

Silicon heterojunction (SHJ) solar cell technology currently holds the world record for silicon based photovoltaic energy conversion. Panasonic has achieved a record efficiency of $25.6\,\%$ with their Heterojunction with Intrinsic Thin film (HIT) solar cell using an interdigitated back contacted design. [1] The fundamental structure of SHJ technology is a crystalline silicon (c-Si) wafer that is passivated on both sides with intrinsic hydrogenated amorphous silicon (a-Si:H). Doped a-Si:H films are deposited on either side of the a-Si:H/c-Si/a-Si:H stack to form the emitter and back surface field. Though this structure produces high quality solar cells, physical understanding of the a-Si:H/c-Si interface still presents challenges. This is shown by the complex models that are used to attempt to describe the current transport methods through the c-Si/a-Si:H interface. [2], [3] One area of this physical understanding is in the defects at the c-Si/a-Si:H interface.

The bulk absorber of SHJ solar cells is a c-Si wafer that is grown through the float-zone (FZ) or Czochralski (Cz) method. C-Si defects have been very well studied and described in the past. [4] Light induced degradation (LID) does occur in crystalline silicon absorbers, but this is typically only with p-type wafers with boron-oxygen interstitial defects. [5] While the bulk of c-Si has a well defined crystalline lattice, dangling bonds (DBs) at the surface increase the surface recombination velocity and need to be passivated prior to adding the doped layers necessary to form the p-n junction and back surface field for solar cell operation. [6] In SHJ solar cells, the surface of the c-Si is passivated with intrinsic a-Si:H as it has fewer defects than doped a-Si:H. Adding a thin layer of a-Si:H, therefore, results in a lower surface recombination velocity and thus, a higher open-circuit voltage (V_{OC}) for a working SHJ device. [7]

The a-Si:H, used for passivation, is a disordered material with defect densities of 10^{16}-10^{19} cm^{-3}. [8] The defects can consist of contamination defects, DBs and vacancy defects among others. [9] Some defects in a-Si:H are metastable, meaning that defect densities in a-Si:H are increased through LID, but can decrease again through annealing. This significantly alters the quality of a-Si:H as a photovoltaic material and this change is known as the Staebler-Wronski effect (SWE). [10] Various models have been applied to explain the SWE, however there is still no consensus on the fundamental mechanisms at hand. [11], [9], [12] One theory is that DBs become unpassivated during light soaking, though more recent research has shown that the nanostructure of the a-Si:H, such void surfaces, plays a role in SWE as well. [12], [13] The a-Si:H/c-Si interface is affected by the surface properties of the c-Si as well as the quality of the passivating a-Si:H layer. [14]

One established way to monitor the quality of a-Si:H passivation of c-Si wafers is to use photoconductance decay (PCD) lifetime measurements. This method probes the interface by measuring the effective minority carrier lifetime (τ_{eff}) in a c-Si wafer or full device. [7] Since the recombination is dominated by the surface, the measurement can be directly related to the quality of the a-Si:H/c-Si interface. [15] In general, higher lifetimes measured in this way suggest a better quality interface and a device with a higher open circuit voltage (V_{OC}). [16]

Utilizing this method, work De Wolf et al. has shown that the τ_{eff} of silicon heterojunction structures change through light soaking. [17], [18] This change in τ_{eff} has been linked strictly to DB generation using a model on the amphoteric nature of dangling bonds in SHJs. [19] The process has been shown to be partially reversible through annealing. [20] Mahtani et al. has shown that there can also be light-induced improvement in τ_{eff}. [21] In this paper the light-induced improvement of τ_{eff} was linked solely to the intial τ_{eff} (τ^0_{eff}) where samples with a low τ^0_{eff} exhibit light-induced improvement and samples with a high τ^0_{eff} exhibit LID. The measurement procedure used in these studies is described in this manuscript as multiple exposure photoconductance decay (MEPCD). In these measurements, hundreds to thousands of PCD measurements are taken in order to study the change in τ_{eff}, and thus the change in a-Si:H/c-Si interface passivation quality upon light exposure.

The study of the light-induced effects on the a-Si:H/c-Si interface passivation quality is studied further here by expanding the deposition parameters of the a-Si:H and the preparation steps of the c-Si wafers. Though changes in passivation quality have been previously attributed solely to c-Si surface DB density increase (N_{S}), results in this manuscript show that this is not always the case. By changing a-Si:H deposition conditions, further insight is gained regarding the mechanisms of these light-induced effects. Results here show that generation of DBs at the interface is not sufficient to explain the changes that are observed and that other factors such as fixed charge can play a significant role depending on which set of sample preparation parameters are used. Furthermore, the results presented here provide further insight into the mechanisms of light-induced improvement in τ_{eff}.

To expand further on these light-induced effects on the τ_{eff} of SHJ structures, doped layers to make both an emitter and a back surface field (BSF) are added. A similar investigation has been done by Mahtahni et al. [21] Here, only the emitter was explored and increases in τ_{eff} were observed. Furthermore, only long time scales were explored in the work of Mahtani, while previous work has shown that there are a lot of light induced changes on very short timescales. [18] This work uses c-Si wafers passivated with a-Si:H using thicknesses close to what are used in SHJ devices and uses doped layers and investigates the short time scales immediately after annealing.

II. Experimental Details

A. Sample deposition

The samples in this work were deposited on $\sim 280\,\mu\mathrm{m}$ thick, ~ 4.0 cm, double polished, FZ c-Si wafers. Phosphorus-doped (n-type) wafers with $\langle 111 \rangle$ orientation were used. The cleaning procedure consisted of $10\,\mathrm{min}$ of $99\,\%$ $\mathrm{HNO_3}$ at room temperature followed by $10\,\mathrm{min}$ of $69\,\%$ $\mathrm{HNO_3}$ at $105\,^{\circ}\mathrm{C}$ to encapsulate organic contaminants in an oxide layer. After this, the oxide was stripped away by a dip in a solution of $0.55\,\%$ HF for $75\,\mathrm{s}$. The a-Si:H layers were deposited by radio

frequency (RF) plasma enhanced chemical vapor deposition (PECVD) at 13.56 MHz. The depositions were carried out at a substrate temperature of 180 °C unless otherwise specified. Thicknesses were verified using spectroscopic ellipsometry (SE).

The intrinsic a-Si:H films were deposited using two sets of deposition conditions. The first set of conditions, referred to here as undiluted, was deposited at 0.7 mbar, 40 sccm SiH_4 and at a power density of 0.015 W cm^{-2}. The second set of conditions, referred to here as diluted, was deposited at 8 mbar, 4 sccm SiH_4, 200 sccm H_2 and at a power density of 0.056 W cm^{-2}. This second set of high-diluted material has been known to produce thin film solar cells with a high V_{OC} and provides good passivation for SHJ solar cells. [22], [23], [24]

The doped a-Si:H layers were deposited using the optimized conditions of Zhang. [25] The p-layer used was deposited at 0.7 mbar, 20 sccm SiH_4 and 3 sccm of B_2H_6 at a power density of 0.021 W cm^{-2}. The n-layer used was deposited at 0.6 mbar, 40 sccm SiH_4 and 11 sccm of PH_3 at a power density of 0.021 W cm^{-2}.

B. Lifetime measurements

τ_{eff} measurements were carried out using a Sinton WTC-120 photoconductance decay setup. This setup uses a light flash that is filtered to only allow red/infrared light to pass through. The spectrum for the measurement flash is given in Figure 1a. This spectrum was measured using an AVANTES Dual AvaSpec 2048. The lifetime measurements at an excess charge carrier density of 10^{15} cm^{-3} is used here.

Figure 1b shows the generation profile of the top a-Si:H layer and the c-Si bulk layer under illumination of the measurement flash. There is also a rear layer of a-Si:H, which is not represented in the figure because the vast majority of the light, in either case, is absorbed before it reaches the rear a-Si:H layer and thus the absorption there is negligible. This generation profile were calculated using the Advanced Semiconductor Analysis (ASA) software developed by the Delft University of Technology's Photovoltaic Materials and Devices (PVMD) group. [26] The optical properties of both a-Si:H and c-Si were obtained using SE.

In order to ascertain the light-induced changes in τ_{eff}, so-called MEPCD measurements were carried out. This means that post-deposition, samples were annealed for two hours at 130 °C. Following this annealing step, the samples were measured over 1000 times consecutively by the PCD measurement tester. The flashes used in the measurement are the light-soaking source.

C. Fourier transform infrared spectroscopy

Fourier Transform Infrared Spectroscopy (FTIR) was used to characterize a-Si:H films. In these cases, the same deposition conditions that were used to make a sample for MEPCD measurements were used to deposit a 100 nm thick a-Si:H layer on top of a Cz, single side polished wafer. FTIR measurements were carried out using a Thermo Fisher Nicolet 5700 FTIR spectrometer in transmittance mode.

Prior to fitting the FTIR measurements, the background is corrected by removing a third order polynomial. The fitting used is a deconvolution of the FTIR response into two Guassian curves. The curve in the range of 1995-2005 cm^{-1} is known as the low-stretching mode (LSM) while the curve with a peak in the range of 2080-2090 cm^{-1} is known as the high stretching mode (HSM). [27] Responses in the LSM correspond to hydrogen which is incorporated into small volume deficiencies such as divacancies and is therefore assigned to monohydrides. [28]. The HSM, on the other hand can be attributed both to monohydrides and higher dihydrides on inner surface voids in a clustered form. [20], [29]

Information about the microstructure of the a-Si:H films used for passivation can be extracted from FTIR measurements using the assumed contributions to the LSM and HSM given above. This can be done using the microstructure parameter R^* as:

$$R^* = \frac{I_{\text{HSM}}}{I_{\text{HSM}} + I_{\text{LSM}}} \tag{1}$$

where I_{HSM} and I_{LSM} are the peak integrals of the HSM and LSM respectively. [22], [24] In general, a higher R^* parameter corresponds to a film with a higher void density, or a more porous film.

In addition to this the atomic percentage of hydrogen (C_{H}) was calculated by using the wagging mode at 640 cm^{-1}. The peak at 640 cm^{-1} was integrated and multiplied by the conversion factor of 1.6×10^{19}. [9]

III. Results and Discussion

The experiments in this section are split into two sections. The first section gives results on MEPCD studies on c-Si passivated with a-Si:H. In this case, undiluted a-Si:H is used and the a-Si:H thickness is 30 nm. Different deposition temperatures are used to modify the microstructure of the a-Si:H to determine the effect of microstructure on the light-induced changes in τ_{eff}.

This is followed by a section on the addition of doped a-Si:H layers. Here the total a-Si:H thickness, including both the passivating intrinsic layer and the doped a-Si:H layers is 14 nm. In this case diluted a-Si:H is used for the intrinsic layer as it has better passivation qualities. [23]

A. Intrinsic Only Study

Figure 2 shows an MEPCD measurement done on an n-type c-Si wafer passivated with undiluted a-Si:H. Though one measurement is presented here, this shape of τ_{eff} evolution upon measurement flashes was exhibited by many different samples. Due to the light flashes of the PCD setup the τ_{eff} of the passivated wafer decreases for the first 100 flashes and then starts to recover and even exceed the initial, post-annealed τ_{eff}. Experiments were also run using an external, white LED as a light source while varying the light soaking time. Here, significant generation was present in the a-Si:H layers as there were more photons in the range above the bandgap of a-Si:H. However, the changes in τ_{eff} were relatively similar with a degradation to around the same relative amount

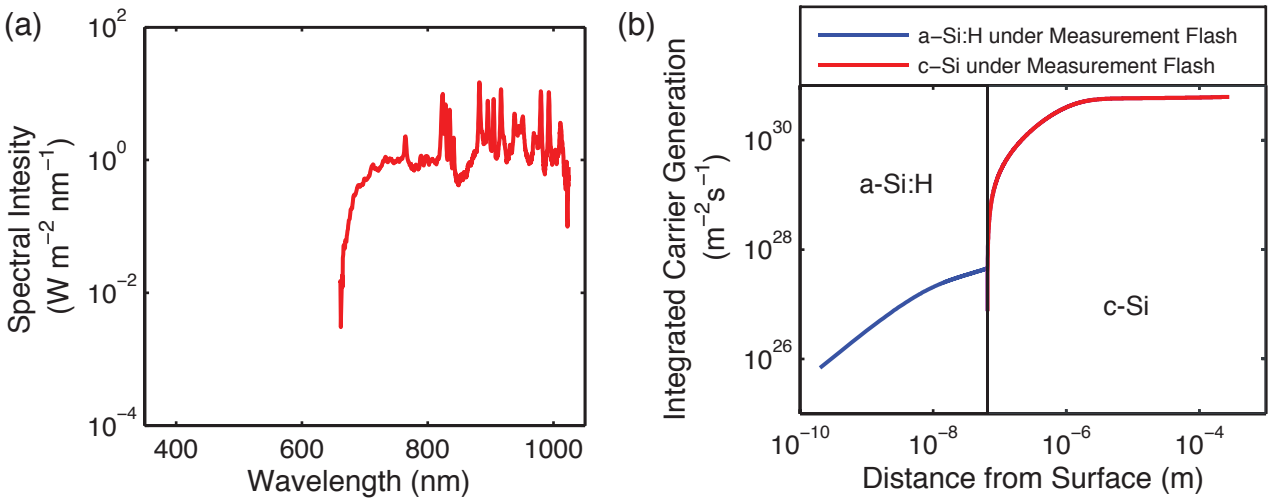

Fig. 1. (a) Light spectrum of flash of Sinton PCD lifetime tester. (b) Cumulative generation profile of samples. The generation profile has been integrated to show how many charge carriers per cm^2 are generated in the a-Si:H film and the c-Si wafer.

with an increase at longer light soaking times. Results without the white LED are shown here as they were more controlled and allowed for a more straightforward analysis to explain the results. It should also be noted here that this measurement, and all MEPCD measurements shown here, can be repeated by annealing. That is to say that if the sample is annealed again at 150 °C for a half hour and the MEPCD measurement is repeated, very similar kinetics will be exhibited again.

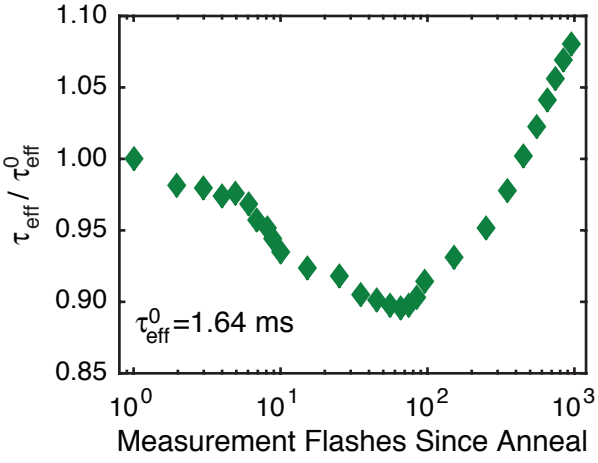

Fig. 2. MEPCD measurement on an n-type ⟨111⟩ wafer passivated by undiluted a-Si:H. No external light soaking is used here.

This measurement presents two important findings. Firstly that, contrary to what was observed by De Wolf et al. samples prepared here on n⟨111⟩ wafers can, indeed, exhibit significant kinetics upon light soaking. [18] Furthermore, this result shows that light induced improvement of τ_{eff} occurs at longer light exposures. In order to investigate the cause of light induced improvement of τ_{eff}, variations on the deposition temperature of the a-Si:H film was carried out.

Changes in the deposition temperature of the passivating a-Si:H film are investigated here. Deposition temperature was chosen as a varying parameter because it is known to affect the microstructure of a-Si:H. [9] The microstructure of the a-Si:H films are measured using FTIR as shown in Figure 3a.

TABLE I
PEAK POSITION (ω) AND PEAK INTEGRAL (I) OF LOW STRETCHING MODE (LSM) AND HIGH STRETCHING MODE (HSM) OF FTIR CURVES FROM FIGURE 3A AT DIFFERENT DEPOSITION TEMPERATURES (T_{DEP}). R^* IS THE MICROSTRUCTURE PARAMETER FROM EQUATION 1. C_{H} IS THE ATOMIC PERCENTAGE OF HYDROGEN CALCULATED FROM THE WAGGING MODE.

T_{dep} [°C]	ω_{LSM} [cm^{-1}]	I_{LSM} [cm^{-1}]	ω_{HSM} [cm^{-1}]	I_{HSM} [cm^{-1}]	R^*	C_{H} at. %
100	2005	93.63	2077	57.33	0.38	13.1
140	2001	60.14	2079	19.78	0.28	9.0
160	1999	147.54	2081	19.05	0.11	11.5
180	1996	73.66	2081	6.11	0.08	6.6
220	1994	131.62	-	0.00	0.00	7.2

The R^* parameter, as determined by Equation 1 along with the peak position of the high and low stretching modes (ω_{HSM} and ω_{LSM}) are calculated from the FTIR measurements in Figure 3a and given in Table I for the a-Si:H films deposited at different deposition temperatures.

Passivation using these deposition conditions were carried out on n⟨111⟩ wafers. Before looking at the kinetics and how the lifetime evolves due to measurement flashing, the initial lifetimes are observed. Figure 3b shows how the as deposited lifetime varies with deposition temperature as well as how R^* varies with deposition temperature. A clear trend is shown here that more porous materials provided poorer passivation. This is in agreement with other studies who have shown that voids in a-Si:H films show them to be poor passivation materials. [14]

These samples were annealed at 150 °C for 2 h and then flashed 1000 times in the dark. The results of this experiment are shown in Figure 3c. These results can be split into three regimes where the samples prepared at 100 °C and 140 °C exhibit lifetime kinetics that are dominated by light induced

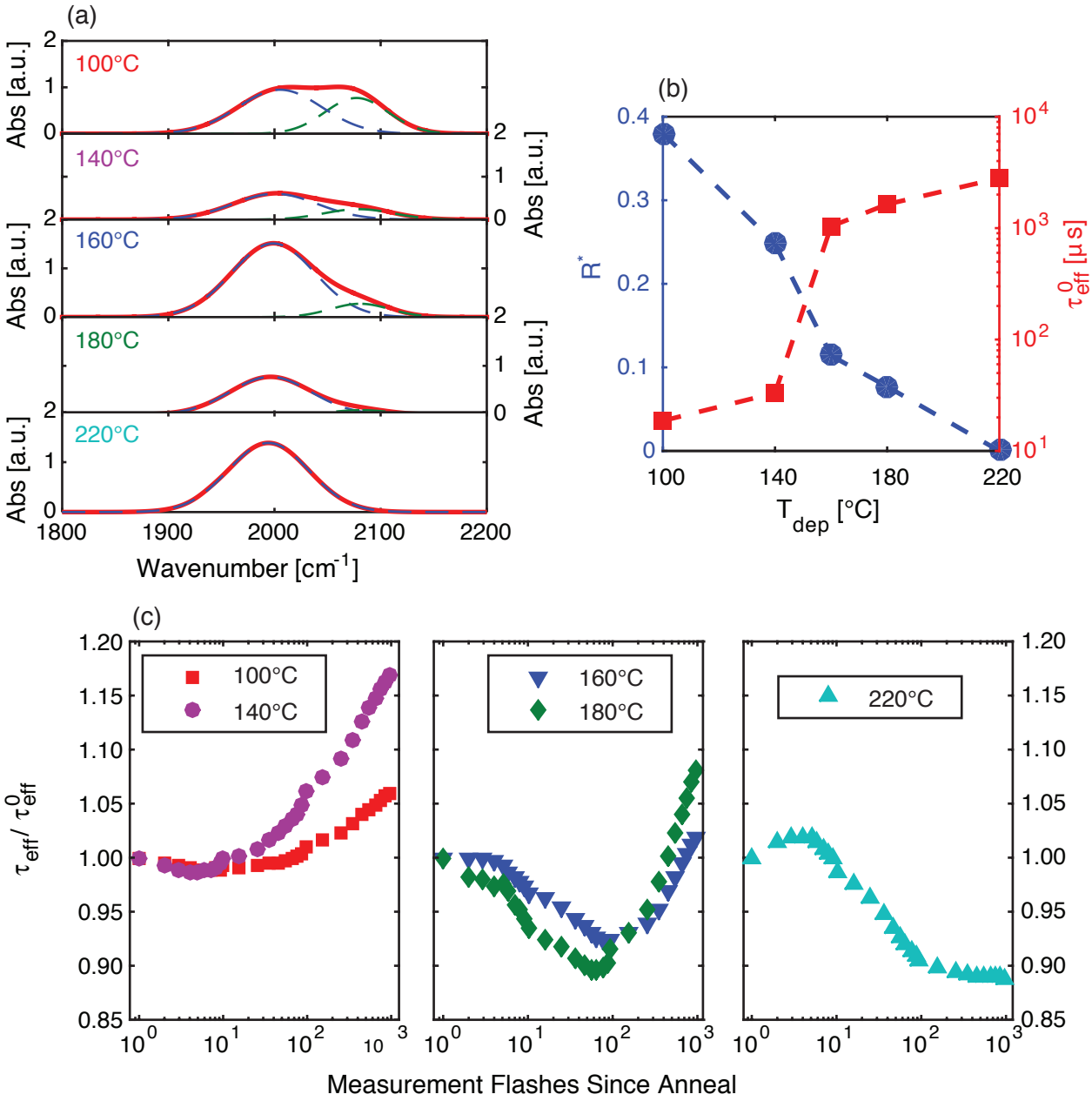

Fig. 3. (a) FTIR measurements on c-Si/a-Si:H interface where a-Si:H was deposited at different deposition temperatures (T_{dep}). Substrate temperature was varied from 100 °C to 200 °C. (b) R^* parameter calculated from FTIR measurements as well as initial lifetime vs deposition temperature. (c) MEPCD measurements on samples with different temperatures. Three panels with different kinetic regime are shown. Leftmost corresponds to samples with $R^* > 0.25$, center corresponds to samples with $0 < R^* < 0.25$, rightmost corresponds to a sample where $R^* \approx 0$.

increases in τ_{eff}, the sample prepared at 220 °C exhibits lifetime kinetics that are dominated by light induced decreases in τ_{eff} and the samples prepared at 160 °C and 180 °C exhibit lifetime kinetics with a light induced decrease followed by a light induced increase in τ_{eff}.

These kinetic regimes can be linked to the R^* parameter of the a-Si:H films as shown in Figure 3b. The C_H of the films is also provided in Table I. The values here change between 7.2 % and 13.1 % but do not correlate with kinetics. As nothing else was varied in the deposition parameters, this suggests that the microstructure of the passivating a-Si:H film plays a role in the measurement flash kinetics of the τ_{eff}. The results show that wafers passivated with a-Si:H films with an R^* of more than 0.25, light flashes tend to increase the lifetime. These films are more porous than ones with a lower R^*. In wafers passivated by a-Si:H films with an R^* of 0, which are dominated by smaller volume deficiency defects such as vacancy defects, the τ_{eff} primarily degrades. Finally when wafers are passivated with medium dense films with an R^* above 0 but less than 0.25, the kinetics the τ_{eff} decreases followed by an increase after around 100 flashes. In these films there are a detectable amount of voids in the films but significantly less than those

TABLE II
SAMPLE DESCRIPTIONS AND AS DEPOSITED τ_{EFF} VALUES

Stack	Name	As Deposited τ_{eff} [ms]
i/c-Si/i	Control	2.3
p/i/c-Si/i	Emitter	2.2
n/i/c-Si/i	BSF	2.6
p/i/c-Si/i/n	Precursor	3.9

in the more porous regime.

This suggests that a possible explanation for the light induced increase in τ_{eff} observed on samples using n-type wafers comes from voids in the passivating a-Si:H films, while the degradation is linked to vacancies in the films. The decay in τ_{eff} can be explained, as has been in literature, by DB formation at the a-Si:H/c-Si interface. This would imply that the quality of chemical passivation is decreased. [18] Though the exact mechanism of the increase in τ_{eff} cannot be fully explained by the results here, one possible explanation is that there is a positive charge build up at the interface. As charge carriers enter the a-Si:H film, defects at the void surface may charge positively and this build up of charge would repel the minority charge carriers of the n-type c-Si wafer (holes) from the interface back into the high lifetime bulk of the n-type c-Si wafer. This would, in essence, increase the lifetime of generated holes in the interface. This effect implies that the light induced changes affect the field-effect passivation of the samples. To investigate this further, MEPCD measurements were carried out using samples with additional doped layers.

B. Doped Layer Studies

To further explore the light induced effects on the a-Si:H/c-Si interface, doped layers were added to monitor their effect on the light-induced kinetics on τ_{eff} observed above. Four distinct samples were deposited. These are given in Table II. Schematics shown in Figure 4. The intrinsic a-Si:H used in this work was the diluted a-Si:H as at this point in the experiments it was found that this material achieved higher τ_{eff} values and became the standard for the research group. [23] The substrate temperature during a-Si:H deposition in these experiments was 180 °C.

Figure 5 shows the MEPCD measurements performed on the control, emitter and BSF samples. The τ_{eff} of the BSF sample decreases with measurement flashes while the τ_{eff} of the emitter sample increases with measurement flashes. The result of this experiment suggest that doped a-Si:H layers do, indeed, affect the lifetime kinetics upon light soaking. This suggests that the BSF sample is dominated by an N_S increase upon light soaking while screening out void charging effects while the emitter sample is dominated by void charging effects while screening out N_S effects. Further analysis about the causes of these screening effects by doped layers is given in Section IV.

In Mahtani et al.'s work, a similar experiment is done and similar results are exhibited. [21] Here, the improvement in samples with an emitter had three possible explanations. The first explanation is that a defect gradient is imposed due to a higher concentration of defects in the p-type layer compared

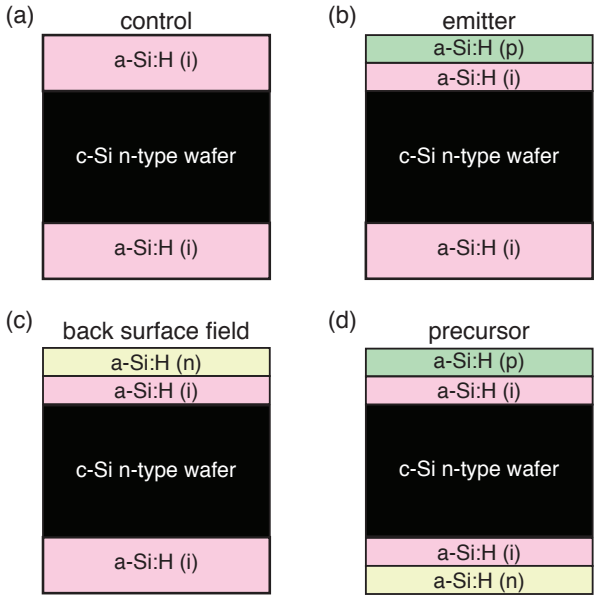

Fig. 4. Schematics of the samples used in this work. (a) the standard sample with 14nm of passivating a-Si:H on either side of the c-Si wafer. (b) the sample with a deposited emitter on one side of the sample. (c) the sample with a deposited back surface field on one side of the sample. (d) full precursor of a SHJ solar cell with both an emitter and a back surface field.

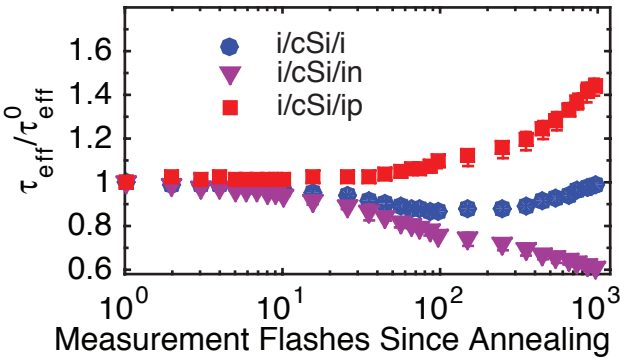

Fig. 5. MEPCD measurement on i/c-Si/i stack, emitter stack and BSF stack.

to the intrinsic layer at the surface of the c-Si wafer. Changes in this gradient due to recombination at the surface may cause interface defects to change in different ways than if there is just an intrinsic layer. However, this explanation would not distinguish between a defect gradient with n-type doping and p-type doping. In this work it is shown that the type of doping has an effect on the kinetics, and light-induced improvement only occurs when p-type doping is applied.

In their case, there was a difference in thickness between their sample with just an intrinsic a-Si:H layer and the one with a p-type layer stack. They claimed that this may be a contribution to the difference in light induced change kinetics, but as this was held constant in the experiments shown here, that explanation does not seem to hold.

Finally, they explain the results claiming that the change in electric field due to the doped layer may have an effect.

This may change the rate of movement of defects during formation. This last example is the only one that is valid for the results shown from these experiments. Therefore our results, in conjunction with the analysis of Mahtani et al., suggest that the electric field induced by the emitter layer is the primary cause of light induced improvement of τ_{eff} upon light soaking.

The next step, after adding a single doped layer to the sample, was to produce a complete SHJ precursor. A p-type, a-Si:H layer is on one side of the sample to form the emitter and an n-type, a-Si:H layer is on the other side forming the BSF. When these samples are first exposed to MEPCD measurements, the lifetime tends to increase with measurement flashes. In this case, the side exposed to light was on the emitter (p-type) side of the sample. This sample was annealed again and exposed to the measurement flashes flipped over with the back surface field (n-type) side exposed. In this second run the kinetics were dominated by a decrease in lifetime. This is shown in Figure 6a. In Figure 6b the experimental order was reversed. Here, the back surface field side was flashed on the first anneal after deposition and then after the second anneal the emitter side was flashed. The kinetics were consistent with the first experiment showing that the flashing side, not the number of annealing cycles, determined whether τ_{eff} would increase or decrease upon light exposure.

IV. Analysis

To explain how void charging can have an influence on the minority carrier lifetime, a band diagram of the a-Si:H/n-type c-Si interface is given in Figure 7. The band diagrams were calculated using the modeling software, AFORS-HET. [30] The digram shows the inversion layer where the band bending in the n-type c-Si will cause holes to drift towards that interface. This is combined with a barrier caused by the valence band offset between the a-Si:H and the c-Si. This could result in a build up of holes at the interface which would cause a positive charging effect at that interface.

Understanding what causes the different light-induced effects in the samples with doped layers starts with the potential effects of light exposure on samples. Firstly there is the generation of charge carriers in the different materials involved in the sample. A calculation of the generation profile is given in Figure 1b. There is significantly higher cumulative generation in the c-Si wafer than in any either of the a-Si:H passivation layers here. There is also generation in the top a-Si:H with very little generation in the rear a-Si:H layer as most of the light has already been absorbed by the c-Si wafer. The second impact of this effect is recombination. In literature, recombination of light-excited carriers is widely given as the cause of the defect density increase in a-Si:H which happens during the Staebler-Wronski Effect. [31], [32] As cumulative generation is orders of magnitude higher in the c-Si wafer, and the diffusion length of minority and majority charge carriers are orders of magnitude higher than wafer thicknesses used here, recombination should occur in relatively equal amounts at both the front and rear side of the sample. Therefore the a-Si:H layers at the front side have more generation than the a-Si:H at the rear of the sample but with roughly the same rates of recombination.

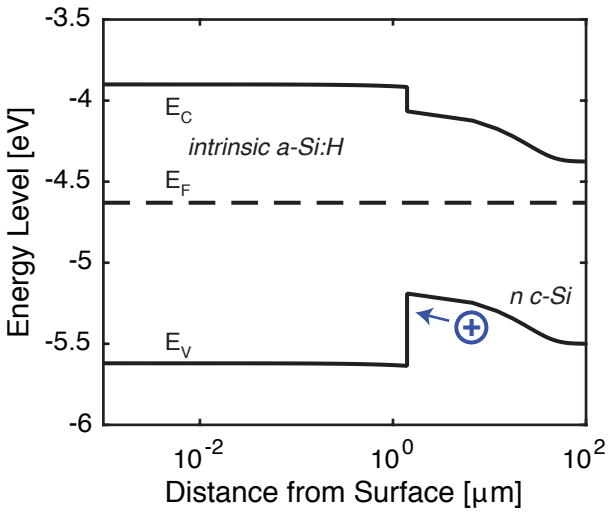

Fig. 7. Band diagram of the c-Si/a-Si:H interface using n-type c-Si and intrinsic a-Si:H. Bands were calculated using the modeling software, AFORS-HET. Hole pictured at the left of the c-Si to show the capability of trapping at the interface.

TABLE III
Effects that are apparent upon light exposure among different samples

Stack	Name	N_S Increase	Void Charging
i/c-Si/i	Control	xx	x
p/i/c-Si/i	Emitter		xx
n/i/c-Si/i	BSF	xx	
p/i/c-Si/i/n	Precursor (p-illumination)		xx
n/i/c-Si/i/p	Precursor (n-illumination)	xx	x

Table III shows which samples exhibit which effects. Samples that exhibit light induced decreases in τ_{eff} have ticks in the "N_S Increase" column and samples that exhibit light induced increases in τ_{eff} have ticks in the "Void Charging" column. This table shows that light-induced N_S increases heavily affect samples except those with a p-layer and when the p-layer is illuminated. This suggests that the field effect caused by the p-layer either screens away the N_S increase, or amplifies the charging in the a-Si:H. To explore this further, the band diagram of the emitter side of the sample is given in Figure 8. Photogenerated holes in c-Si drift towards the a-Si:H/c-Si interface while being blocked by the heterojunction at the inversion layer just as in the sample with only intrinsic material shown in Figure 7. This could explain the build up of positive charge at the interface that increases the τ_{eff}. That built up positive charge changes the band structure as shown in Figure 8 and thusly increases τ_{eff}.

The addition of a BSF has the opposite effect of the emitter. With the BSF sample, τ_{eff} degrades without any corresponding increase in τ_{eff} caused by positive void charging. This fits with the explanation that photogenerated holes may cause the positive charging in voids in a-Si:H as the BSF would screen away photogenerated holes in the a-Si:H and block photogenerated holes from the c-Si wafer. The band diagram of the BSF of a SHJ solar cell is given in Figure 9. Photogenerated electrons

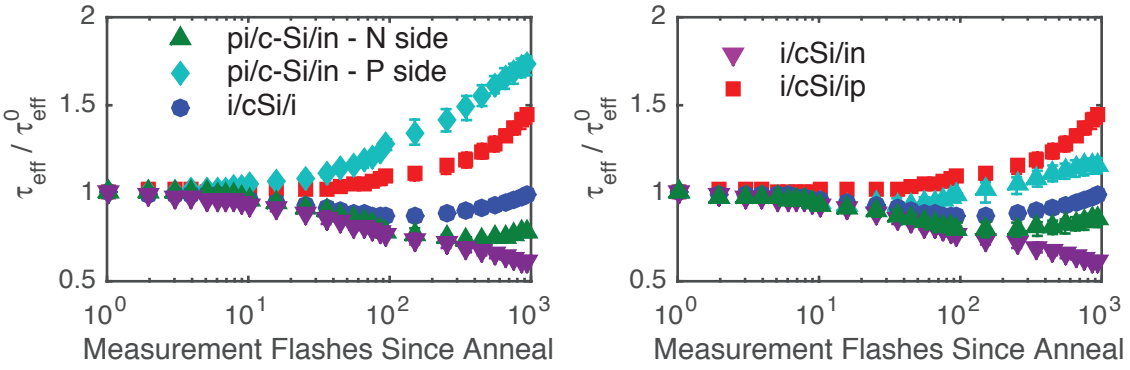

Fig. 6. MEPCD measurement on precursor stack as well as other stacks shown in Figure 5. The two figures presented here obtain the same measurements for the i/i and single doped layer samples. However in the case of the precursor sample, in (a) the emitter side was illuminated first, while in (b) the back surface field side was illuminated first.

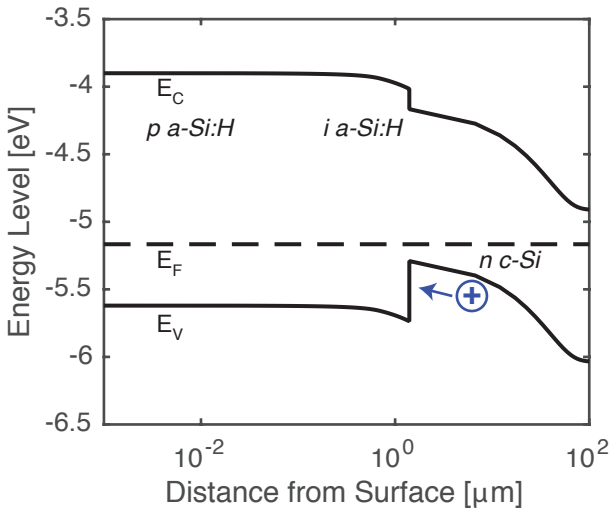

Fig. 8. Band diagram of relevant sections of emitter sample calculated using AFORS-HET. Hole pictured at the left of the c-Si to show the capability of positive charge trapping at the interface.

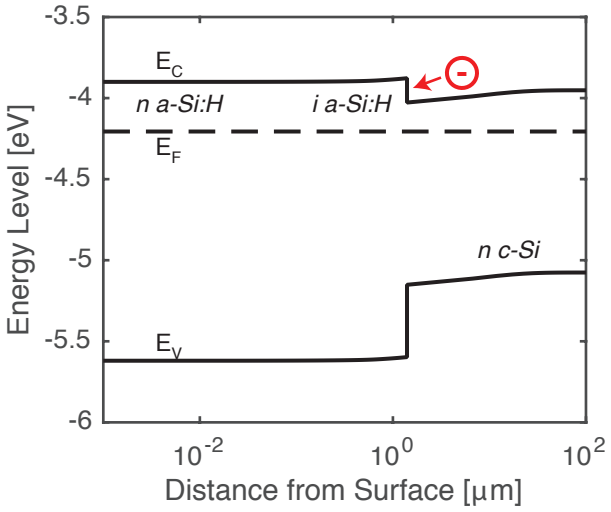

Fig. 9. Band diagram of relevant sections of BSF sample. Electron pictured at the left of the c-Si in the conduction band to show the capability of negative charge trapping at the interface.

in the c-Si will drift towards the a-Si:H/c-Si junction while encountering a barrier from the heterojunction in this case. This may cause a build up of negative charge at the interface which would reduce τ_{eff} in the same way that positive charging increases τ_{eff}.

One potential issue with this explanation is that both the emitter sample and the BSF sample have a single intrinsic a-Si:H layer on the rear side of the wafer. The screening effects of the fields generated by the doped layers should not play any role for the rear side. However, this can be explained by recalling what the τ_{eff} measurements actually represent. In this manuscript they represent the effective lifetime at an injection level of 1×10^{15}. However, this lifetime is based on the reciprocal sums of different lifetime contributions of different parts of the sample. This is expressed as:

$$\tau_{\text{eff}} = \left(\frac{1}{\tau_{\text{bulk}}} + \frac{1}{\tau_{\text{front}}} + \frac{1}{\tau_{\text{rear}}} \right)^{-1} \tag{2}$$

Where τ_{bulk} is the bulk lifetime, τ_{front} is the front surface lifetime and τ_{rear} is the rear surface lifetime. Because of the nature of this reciprocal addition, if the three lifetimes are of very different values, the lowest value dominates. Here $\tau_{\text{bulk}} >> \tau_{\text{front}}$ and $\tau_{\text{bulk}} >> \tau_{\text{rear}}$ at the injection level of $1 \times 10^{15}\,\text{cm}^{-3}$. Therefore, τ_{eff} is dependent mainly on the surface lifetimes, τ_{front} and τ_{rear}. Similarly, if $\tau_{\text{front}} << \tau_{\text{rear}}$ then the measured τ_{eff} will primarily be based on τ_{front}. In the case of the BSF and emitter samples, the lifetime of the side with the doped layers will likely be lower than the lifetime of the side with the thicker intrinsic layer on the back as the doped a-Si:H adds extra dangling bonds thus increasing the N_S value. Though the field effect of adding doped layers also has an influence on τ_{eff}, an assumption is used here that N_S is a larger factor than additional field effects of doped layers on the surface lifetime. If this assumption holds, τ_{eff} is primarily determined by the lifetime of the side with the doped layer. This explains why the screening of the doped layers have such a significant effect on the τ_{eff} during light soaking even though both void charging and N_S are likely occurring at the rear side

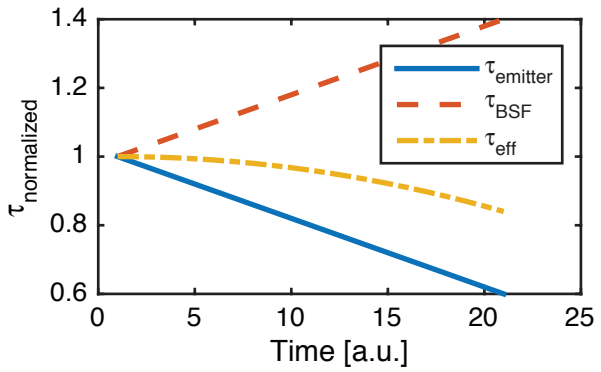

Fig. 10. Calculation of τ_{eff} under the assumption that τ_{emitter} and τ_{BSF} change according to the curves given in Figure 6. Simulated τ_{emitter} and τ_{BSF} is also shown here. τ_{bulk} is ignored so $\tau_{\text{eff}} = \left(\frac{1}{\tau_{\text{emitter}}} + \frac{1}{\tau_{\text{BSF}}}\right)^{-1}$

of the wafer.

Explaining the results of light soaking on precursors begins with isolating the two sides of the sample. Each of these sides have a unique surface lifetime referred to here as τ_{emitter} and τ_{BSF}. If τ_{emitter} and τ_{BSF} are on the same order of magnitude in the annealed state prior to light soaking, then changes to either surface would have a significant effect on τ_{eff}. This assumption is made by the very similar τ_{eff} values measured of the emitter and BSF sample and shown in Table II.

If τ_{eff} is determined by the lifetime at either side equally, and the effects on surface lifetime are primarily caused by recombination at the interface, then there should not be a difference in light soaking kinetics depending on which side is illuminated. This is because due to the high diffusion lengths of high quality c-Si, and the fact that there are orders of magnitude more charge carriers generated in the c-Si, both sides of the sample should have relatively equivalent levels of recombination. The analysis above showed that τ_{emitter} increases upon illumination while τ_{BSF} decreases upon illumination. Assuming the surfaces of the precursors have similar properties as those used in the singled doped layer experiment, both surfaces change at equal but opposite rates when illuminated (the emitter sample reaches a final lifetime of 1.4x the initial lifetime and the BSF sample reaches a final lifetime of 0.6x the initial lifetime). If this were the case in the precursor, one would expect that the τ_{eff} would decrease based on light soaking since the degradation of lifetime would have a greater effect as is shown in Figure 10. In this Figure, τ_{emitter} and τ_{BSF} are reciprocally added together while one decreases and the other increases at the same rate. As can be seen, the resultant sum decreases overall. Since the precursor material does not decrease uniformly, this shows that surface recombination is not the only relevant factor in changing τ_{eff} due to light illumination. The fact that the kinetics are reversed depending on the light soaking side (Figure 6) implies that generation in the a-Si:H must also be playing a role in these kinetics.

This finding is fundamental to understanding the nature of light soaking kinetics of the silicon heterointerface. Prior work has suggested that recombination of light-excited carriers causes the increase in defects in a-Si:H that lead to the SWE. [31], [32] Therefore, since recombination at both sides is relatively equal regardless of the flashing side, the N_{S} increase should be similar regardless of the flashing side. The only difference between the two sides it that the illuminated side has significant charge carrier generation in the a-Si:H while the a-Si:H at rear side of the sample undergoes almost no light induced generation. Though this would not significantly affect the changes in N_{S} it could affect the light induced change in surface charging. This would imply that the negative charging at the BSF and the positive charging at the emitter may only occur when their respective side is flashed. This is because there is significant generation in the a-Si:H. As explained above, the charging can be explained by the accumulation of charge due to drift of charge carriers towards the interface that then experience a barrier at that interface. These barriers are shown in Figures 8 and 9. These results suggest that this charging that has long term effects on τ_{eff} may only occur when there is saturated carrier generation in the a-Si:H layers. Therefore the side being flashed has a dominant effect when charging of one side would cause an increase in τ_{eff} and charging of the other side would have a decrease in τ_{eff}. This explanation of charging on illuminated sides of the sample explains why there is not the expected behavior in Figure 10 and why the flashed side dominates the τ_{eff} kinetics.

V. Conclusions

This manuscript has shown an investigation of the light induced degradation and increase of the τ_{eff} of c-Si wafers passivated with a-Si:H. It has been shown that in the case of n-type wafers, light soaking tends to decrease the τ_{eff} when the passivating film is dense and tends to increase the τ_{eff} when the passivating film is porous. The light-induced increases in τ_{eff} suggest that DB formation at the c-Si/a-Si:H interface is not the only factor at play and a build up of positive charge, in the case of porous films passivating n-type wafers, may also play a role in these kinetics.

Furthermore, this work investigated the effect of doped a-Si:H layers on the metastable kinetics of the light induced changes to passivation quality. When a p-type layer is added, the sample exhibits only light induced increases in τ_{eff}, while an n-type layer shows kinetics dominated by a decrease τ_{eff} upon light exposure. This has shown that doped layers do, in fact, have an influence on the light-induced effects of the silicon heterostructure. Though similar work had been carried out in the past, this, more extensive study, has ruled out possible explanations for the increase in lifetime caused by the p-type layer leaving only the explanation that the electric field generated at the a-Si:H interface may be influencing the lifetime kinetics. These results help to isolate the two effects of light soaking on a SHJ sample, which are an increase of N_{S} that decreases lifetime and a positive charging of voids in the material that increases lifetime.

Finally, full SHJ precursors that had both a p-type emitter and an n-type back surface field were exposed to MEPCD measurements. The experiments showed that the sample followed similar kinetics to those of the single doped layers and

this depends on which side the sample is flashed on. Whereas previously the effects were isolated with only a BSF or only an emitter, these samples had both. The fact that the kinetics of the lifetime changes due to light soaking depend on the flashing side suggest that charging only occurs when a-Si:H has sufficient generation.

ACKNOWLEDGMENT

The authors of this paper would like to acknowledge Martijn Tijssen, Stefan Hierman, Remko Koornneef and Kasper Zweetsloot for their invaluable technical assistance on all aspects of this project. Furthermore the authors would like to acknowledge Jimmy Melskens for insightful comments and suggestions during the course of this study. This project was done through the funding of STW in the Fundamentals of Silicon Heterojunctions (FLASH) consortium in the Netherlands under the grant number 12166.

REFERENCES

[1] Panasonic, "Panasonic HIT Solar Cell Achieves World's Highest Conversion Efficiency of 24.7% at Research Level," Osaka, Japan, feb 2013. [Online]. Available: http://panasonic.co.jp/corp/news/official.data/data.dir/2013/02/en130212-7/en130212-7.html

[2] Y. Song, M. Park, E. Guliants, and W. Anderson, "Influence of defects and band offsets on carrier transport mechanisms in amorphous silicon/crystalline silicon heterojunction solar cells," *Solar Energy Materials and Solar Cells*, vol. 64, pp. 225–240, 2000. [Online]. Available: http://www.sciencedirect.com/science/article/pii/S0927024800002221

[3] T. F. Schulze, L. Korte, E. Conrad, M. Schmidt, and B. Rech, "Electrical transport mechanisms in a-Si:H/c-Si heterojunction solar cells," *Journal of Applied Physics*, vol. 107, no. 2, p. 023711, 2010. [Online]. Available: http://scitation.aip.org/content/aip/journal/jap/107/2/10.1063/1.3267316

[4] G. D. Watkins, "Intrinsic defects in silicon," *Materials Science in Semiconductor Processing*, vol. 3, no. 4, pp. 227–235, aug 2000. [Online]. Available: http://linkinghub.elsevier.com/retrieve/pii/S1369800100000378

[5] J. Schmidt and K. Bothe, "Structure and transformation of the metastable boron- and oxygen-related defect center in crystalline silicon," *Physical Review B*, vol. 69, no. 2, p. 024107, jan 2004. [Online]. Available: http://link.aps.org/doi/10.1103/PhysRevB.69.024107

[6] B. Hoex, J. J. H. Gielis, M. C. M. van de Sanden, and W. M. M. Kessels, "On the c-Si surface passivation mechanism by the negative-charge-dielectric Al[sub 2]O[sub 3]," *Journal of Applied Physics*, vol. 104, no. 11, p. 113703, 2008. [Online]. Available: http://link.aip.org/link/JAPIAU/v104/i11/p113703/s1&Agg=doi

[7] R. A. Sinton, "Quasi-steady-state photoconductance, a new method for cell material and device characterization," in *25th PVSC*, 1996, pp. 457–460. [Online]. Available: http://ieeexplore.ieee.org/xpls/abs_all.jsp?arnumber=564042

[8] M. Stutzmann, "The defect density in amorphous silicon," *Philosophical Magazine Part B*, vol. 60, no. 4, pp. 531–546, oct 1989. [Online]. Available: http://www.tandfonline.com/doi/abs/10.1080/13642818908205926

[9] A. H. M. Smets, W. M. M. Kessels, and M. C. M. van de Sanden, "Vacancies and voids in hydrogenated amorphous silicon," *Applied Physics Letters*, vol. 82, no. 10, p. 1547, 2003. [Online]. Available: http://link.aip.org/link/APPLAB/v82/i10/p1547/s1&Agg=doi

[10] D. L. Staebler and C. R. Wronski, "Reversible conductivity changes in discharge-produced amorphous Si," *Applied Physics Letters*, vol. 31, no. 4, p. 292, 1977. [Online]. Available: http://link.aip.org/link/APPLAB/v31/i4/p292/s1&Agg=doi

[11] R. Street, *Hydrogenated amorphous silicon*. Cambridge: Cambridge University Press.

[12] J. Melskens, A. H. M. Smets, M. Schouten, S. W. H. Eijt, H. Schut, and M. Zeman, "New Insights in the Nanostructure and Defect States of Hydrogenated Amorphous Silicon Obtained by Annealing," *IEEE Journal of Photovoltaics*, vol. 3, no. 1, pp. 65–71, jan 2013. [Online]. Available: http://ieeexplore.ieee.org/lpdocs/epic03/wrapper.htm?arnumber=6363507

[13] M. Fehr, A. Schnegg, B. Rech, O. Astakhov, F. Finger, R. Bittl, C. Teutloff, and K. Lips, "Metastable Defect Formation at Microvoids Identified as a Source of Light-Induced Degradation in a-Si:H," *Physical Review Letters*, vol. 112, no. 6, p. 066403, feb 2014. [Online]. Available: http://link.aps.org/doi/10.1103/PhysRevLett.112.066403

[14] S. De Wolf, A. Descoeudres, Z. C. Holman, and C. Ballif, "High-efficiency Silicon Heterojunction Solar Cells: A Review," *Green*, vol. 2, no. 1, pp. 7–24, jan 2012. [Online]. Available: http://www.degruyter.com/view/j/green.2012.2.issue-1/green-2011-0018/green-2011-0018.xml

[15] A. B. Sproul, "Dimensionless solution of the equation describing the effect of surface recombination on carrier decay in semiconductors," *Journal of Applied Physics*, vol. 76, no. 5, p. 2851, 1994. [Online]. Available: http://link.aip.org/link/JAPIAU/v76/i5/p2851/s1&Agg=doi

[16] S. De Wolf and M. Kondo, "Nature of doped a-Si:H/c-Si interface recombination," *Journal of Applied Physics*, vol. 105, no. 10, p. 103707, 2009. [Online]. Available: http://link.aip.org/link/JAPIAU/v105/i10/p103707/s1&Agg=doi

[17] S. De Wolf, S. Olibet, and C. Ballif, "Stretched-exponential a-Si:Hc-Si interface recombination decay," *Applied Physics Letters*, vol. 93, no. 3, p. 032101, 2008. [Online]. Available: http://link.aip.org/link/APPLAB/v93/i3/p032101/s1&Agg=doi

[18] S. De Wolf, B. Demaurex, A. Descoeudres, and C. Ballif, "Very fast light-induced degradation of a-Si:H/c-Si(100) interfaces," *Physical Review B*, vol. 83, no. 23, p. 233301, jun 2011. [Online]. Available: http://link.aps.org/doi/10.1103/PhysRevB.83.233301

[19] S. Olibet, E. Vallat-Sauvain, and C. Ballif, "Model for a-Si:H/c-Si interface recombination based on the amphoteric nature of silicon dangling bonds," *Physical Review B*, vol. 76, no. 3, p. 035326, jul 2007. [Online]. Available: http://link.aps.org/doi/10.1103/PhysRevB.76.035326

[20] E. Mahdi, E. Mhamdi, J. Holovsky, C. Ballif, and S. D. Wolf, "Is light-induced degradation of a-Si:H/c-Si interfaces reversible?" *Applied Physics Letters*, vol. 104, p. 252108, 2014.

[21] P. Mahtani, R. Varache, B. Jovet, C. Longeaud, J.-P. Kleider, and N. P. Kherani, "Light induced changes in the amorphous/crystalline silicon heterointerface," *Journal of Applied Physics*, vol. 114, p. 124503, 2013. [Online]. Available: http://dx.doi.org/10.1063/1.4821235

[22] M. Fischer, H. Tan, J. Melskens, R. Vasudevan, M. Zeman, and A. H. M. Smets, "High pressure processing of hydrogenated amorphous silicon solar cells: Relation between nanostructure and high open-circuit voltage," *Applied Physics Letters*, vol. 106, p. 043905, 2015.

[23] D. Deligiannis, R. Vasudevan, A. H. M. Smets, R. A. C. M. M. V. Swaaij, and M. Zeman, "Surface passivation of c-Si for silicon heterojunction solar cells using high-pressure hydrogen diluted plasmas," *AIP Advances*, vol. 5, p. 097165, 2015.

[24] A. H. M. Smets, M. Fischer, and M. Zeman, "Progress in a-Si:H solar cells by a-Si:H nanostructure engineering," in *21st Photovoltaic Science and Engineering Conference*, 2011, pp. 1–2.

[25] D. Zhang, "Surface passivation and optical design of silicon heterojunction solar cells," Ph.D. dissertation, 2015.

[26] B. Pieters, J. Krc, and M. Zeman, "Advanced numerical simulation tool for solar cells-ASA5," *Conference Record of the 2006 IEEE 4th World Conference on Photovoltaic Energy Conversion*, pp. 1513–1516, 2006. [Online]. Available: http://ieeexplore.ieee.org/xpls/abs_all.jsp?arnumber=4059936

[27] J. Melskens, A. H. M. Smets, S. W. H. Eijt, H. Schut, E. Brück, and M. Zeman, "The nanostructural analysis of hydrogenated silicon films based on positron annihilation studies," *Journal of Non-Crystalline Solids*, vol. 358, no. 17, pp. 2015–2018, sep 2012. [Online]. Available: http://linkinghub.elsevier.com/retrieve/pii/S002230931200052X

[28] S. Chakraborty and D. Drabold, "Static and dynamic properties of hydrogenated amorphous silicon with voids," *Physical Review B*, vol. 79, no. 11, pp. 1–8, 2009.

[29] A. H. M. Smets and M. van de Sanden, "Relation of the Si-H stretching frequency to the nanostructural Si-H bulk environment," *Physical Review B*, vol. 76, no. 7, p. 073202, aug 2007. [Online]. Available: http://link.aps.org/doi/10.1103/PhysRevB.76.073202

[30] R. Varache, C. Leendertz, M. E. Gueunier-farret, J. Haschke, D. Muñoz, and L. Korte, "Investigation of selective junctions using a newly developed tunnel current model for solar cell applications," *Solar Energy Materials and Solar Cells*, vol. 141, pp. 14–23, 2015. [Online]. Available: http://dx.doi.org/10.1016/j.solmat.2015.05.014

[31] M. Stutzmann, W. Jackson, and C. Tsai, "Light-induced metastable defects in hydrogenated amorphous silicon: A systematic study," *Physical Review B*, vol. 32, no. 1, 1985. [Online]. Available: http://prb.aps.org/abstract/PRB/v32/i1/p23_1

[32] R. S. Crandall, "Defect relaxation in amorphous silicon: Stretched exponentials, the Meyer-Neldel rule, and the Staebler-Wronski effect," *Physical Review B*, vol. 43, no. 5, pp. 4057–4070, 1991.